

# The Effect of Intermittent Turbulence on Drop Size in Immiscible Liquid-Liquid Dispersion Mechanically Agitated by High-Shear Sawtooth Impeller

Roman Formánek, Radek Šulc\*

Czech Technical University in Prague, Faculty of Mechanical Engineering, Department of Process Engineering,  
 Technická 4, 160 00, Prague 6, Czech Republic  
 Radek.Sulc@fs.cvut.cz

The effect of intermittent turbulence on drop size reported by Bałdyga and Podgórska (1998) was analysed and the multifractal exponent  $\alpha_{FT}$  was evaluated in a model system of immiscible silicon oil-water dispersion mechanically agitated by a high-shear sawtooth impeller. The  $\alpha_{FT}$  values of approximately 1.64 on average and 1.46 were found for regions close to the impeller and the region outside the impeller, respectively. Finally, the relation between Sauter mean diameter  $d_{32}$  and maximum drop size  $d_{max}$  was investigated. The  $d_{32}/d_{max}$  values of approximately 0.6 on average and 0.5 were found for regions close to the impeller and the region outside the impeller, respectively. The droplet sizes were obtained by the in-situ measurements technique and by the image analysis method.

## 1. Introduction

Dispersed immiscible liquid-liquid systems are usually characterized by the Sauter mean diameter  $d_{32}$  and drop size distribution. Based on Hinze – Kolmogorov theory (Kolmogorov, 1949; Hinze, 1955) and assuming breakup occurring in the inertial subrange of turbulence and local isotropy state, the following relation between maximum stable drop size  $d_{max}$  and impeller Weber number  $We_M$  can be derived (Pacek et al., 1998):

$$d_{max} / D = C_1 \cdot We_M^{-3/5} \quad (1)$$

where  $D$  is the impeller diameter,  $C_1$  is the proportionality constant. The same correlation with the exponent of  $-0.6$  has been expected for the relation between the equilibrium Sauter mean diameter,  $d_{32}$ , and the impeller Weber number, assuming the constant relationship between the Sauter mean diameter  $d_{32}$  and the maximum drop size  $d_{max}$  (Calabrese et al., 1986):

$$d_{32} / d_{max} = C_2 \quad (2)$$

where  $C_2$  is the proportionality constant.

Intermittent turbulence refers to an experimental phenomenon characterized by random changes in the turbulence characteristics in a turbulent flow at the small turbulence scale level at a given location during vortex stretching in the process of turbulent eddy breakup (Bałdyga and Bourne, 1993, 1995). The vorticity and turbulent stresses are not distributed uniformly. These sudden fluctuations in turbulence intensity, whether high or low, even in the case of homogeneous isotropic turbulence, can significantly influence the breakup of the droplets (Bałdyga and Podgórska, 1998).

Low values of the multifractal exponent  $\alpha_{FT} \ll 1$  indicate the presence of peaks in the turbulent energy dissipation rate. However, the probability of these peaks is low. In this case, some turbulent eddies exhibit higher turbulent energy dissipation rate than other, they are “more violent”, but these eddies are not frequent (Bałdyga and Podgórska, 1998).

High values of the multifractal exponent  $\alpha_{FT} > 1$  indicate that the turbulent stresses generated by the acting eddies are smaller than predicted by the Kolmogorov theory of local turbulence (Bałdyga and Podgórska, 1998). Meneveau and Sreenivasan (1989, 1991) reported values of the multifractal exponent in the range  $0.12 < \alpha_{FT} < 1.78$  for turbulence formed in the boundary layer or grid-generated turbulence. She and Levaque (1994) reported a minimum value of  $\alpha_{FT} = 0.33$ . Bałdyga and Bourne (1993) reported that the most probable value of the  $\alpha_{FT}$  exponent is 0.961.

Bałdyga and Podgórska (1998) derived the relation between maximal stable drop size  $d_{max}$  in dilute non-coalescing liquid-liquid dispersion for drop breaking that occurs in the inertial subrange of turbulence and that takes internal intermittency into account:

$$\frac{d_{max}}{D} = C_3 \cdot We_M^{\frac{-0.6}{1-0.4 \cdot (1-\alpha_{FT})}} \quad (3)$$

where  $\alpha_{FT}$  is the multifractal exponent. When the multifractal exponent  $\alpha_{FT}$  equals 1, the exponent of the impeller Weber number in Eq(3) equals -0.6, thus the relation corresponds to the Hinze-Kolmogorov theory assuming a local isotropy state (Bałdyga and Podgórska, 1998).

The question arises of how to determine the maximum drop size,  $d_{max}$ , and whether the  $d_{32}/d_{max}$  ratio is constant as assumed. Formánek and Šulc (2022) tested different ways of estimating  $d_{max}$  using the cumulative frequency drop size distribution. Subsequently, the multifractal exponents  $\alpha_{FT}$  were determined using Eq(3). The proposed methodology was applied for the model dispersion of silicone oil and distilled water agitated by a Rushton turbine. They reported that the correct determination of the maximum drop size is a crucial factor for the correct estimation of the multifractal exponent  $\alpha_{FT}$ . The  $\alpha_{FT}$  values were determined in two regions close to the impeller and one region outside the impeller. The  $\alpha_{FT}$  values of approx. 0.73 and 0.81 were found for regions close to the impeller and the region outside the impeller, respectively.

The contribution aims to apply the procedure proposed by Formánek and Šulc (2022) and to analyse the multifractal exponent  $\alpha_{FT}$  in the model system of silicone oil and distilled water agitated by a high-shear sawtooth impeller using experimental data obtained in our previous work (Formánek and Šulc, 2020). Finally, the relationship between the Sauter mean diameter  $d_{32}$  and the maximum drop size  $d_{max}$  was investigated.

## 2. Methods

### 2.1 Experimental set-up

The experiments were carried out in the fully baffled cylindrical vessel with flat bottom. An immiscible liquid system of distilled water and silicone oil (Wacker AP200) was agitated by a high-shear sawtooth impeller. The physical properties of the immiscible liquid system investigated are presented in Table 2. The vessel was placed in the square optical box which eliminates the image distortion. The droplet sizes were measured in-situ by non-intrusive optical method in three different regions. The experimental device arrangement and placement of the regions of interest are shown in Figure 1. Detailed data are presented in Formánek and Šulc (2020). Drop sizes were measured using the non-intrusive in-situ optical method via image analysis from images captured by a digital camera in a plane illuminated by a light. Drop boundary was identified using pixel shade gradient method (Formanek et al, 2019). The resolution deviation was less than 0.01 % (Formánek and Šulc, 2020).

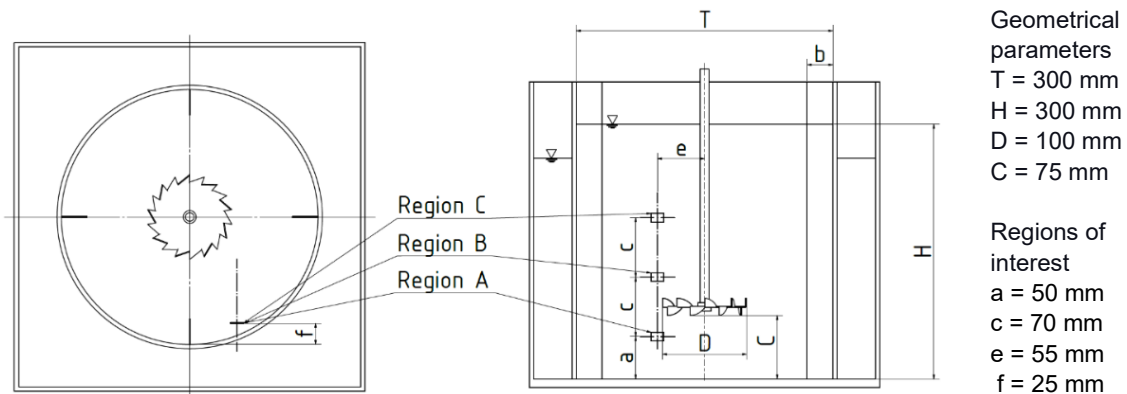


Figure 1: The experimental device arrangement

Table 2: Physical properties of an immiscible liquid-liquid system investigated (temperature  $T = 23.5^\circ\text{C}$ )

Phase	Density <sup>*1</sup> ( $\text{kg m}^{-3}$ )	Dynamic viscosity <sup>*2</sup> ( $\text{mPa s}$ )	Surface tension <sup>*3</sup> ( $\text{mN m}^{-1}$ )	Volumetric fraction (-)
Continuous	997.66	0.94	71.97	0.999 53
Dispersed	1 075.58	223	26.42	0.000 47

Note: <sup>\*1</sup> pycnometer method. <sup>\*2</sup> rotational viscometry (Reotec RC20). <sup>\*3</sup> Krüss Force Tensiometer.

## 2.2 Experimental data

The 10 image sets were captured repeatedly after 5 min; thus the total measurement time was 50 minutes for given region and the impeller rotational speed. When the image sets were captured (each image set consists of 1,000 images), the impeller rotational speed increased by a jump. The experiments were carried out for three impeller rotational speeds: a) 600 rpm ( $Re_M = 102,055$ ), b) 700 rpm ( $Re_M = 119,064$ ), and c) 800 rpm ( $Re_M = 136,074$ ) in three regions of interest. The frequency distribution of drop sizes evaluated for all scanned areas and the impeller rotational speeds are presented in Figure 2 on a logarithmic scale to visualize the time evolution of the drop size distribution. For clearer view, the distribution curves are presented at the initial and final time steps of the measurement (i.e. in the initial time step  $t = 5$  min and at the end of the measurement at time  $t = 50$  min) only.

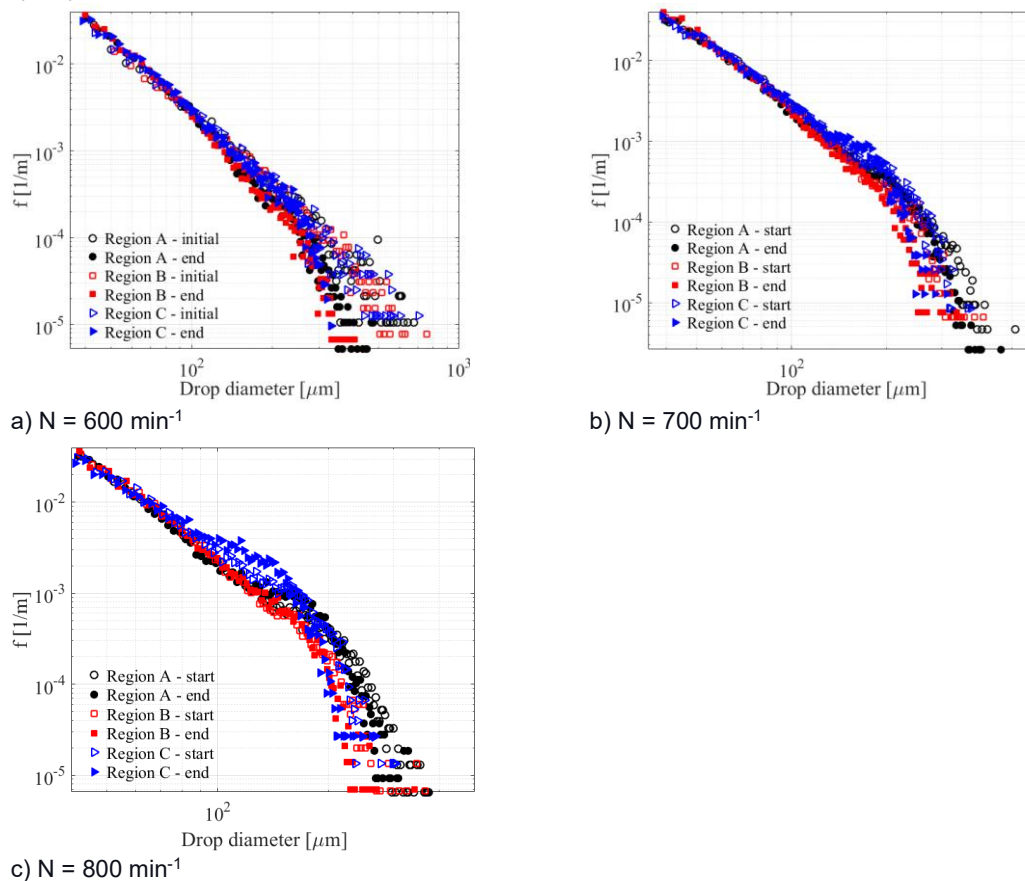


Figure 2: The time development of the frequency drop size distribution: a)  $N = 600 \text{ rpm}$ , b)  $N = 700 \text{ rpm}$ , c)  $N = 800 \text{ rpm}$

For the impeller speeds tested, the drop size distributions remained practically unchanged up to droplet sizes of approximately  $100 \mu\text{m}$ , regardless of the measurement region investigated. Droplet size changes are only visible for larger droplet sizes, in the range of  $200 - 800 \mu\text{m}$  for an impeller rotational speed of  $600 \text{ rpm}$ , and in the range of  $200 - 400 \mu\text{m}$  for higher impeller rotational speeds. Increasing impeller rotational speed, an increase in droplet frequency is also visible in the middle part of the distribution curve, indicating that large droplets are dispersed over time into droplets between  $100 - 200 \mu\text{m}$  in size.

The maximum drop sizes estimated for the cumulative percentage of 95 %, 97 %, 99 %, 99.3 %, 99.5 %, 99.7 %, and 99.9 % from the relative cumulative frequency drop size distribution obtained at the end of a measured

time step for each region and impeller rotational speed were evaluated and selected data are presented in Table 3. For comparison, the maximum drop size was also estimated as an average of 1 % of the number of largest drops (denoted  $d_{99\text{avg}}$ ).

Table 3: The maximum drop sizes estimated

Region	N (min <sup>-1</sup> )	$d_{99}$ ( $\mu\text{m}$ )	$d_{99.3}$ ( $\mu\text{m}$ )	$d_{99.5}$ ( $\mu\text{m}$ )	$d_{99.7}$ ( $\mu\text{m}$ )	$d_{99.9}$ ( $\mu\text{m}$ )	$d_{99\text{avg}}^{*1}$ ( $\mu\text{m}$ )	$d_{\text{mexp}}^{*2}$ ( $\mu\text{m}$ )
A	600	155	163.8	172.1	184.9	213.4	277.2	473.8
	700	148.4	156.6	164.4	176.4	203.1	254.9	464.7
	800	151.2	159.8	167.9	180.6	208.6	227.5	332.2
B	600	147.8	155.8	163.5	175.3	201.3	255.9	410.8
	700	131.3	137.9	144.1	153.5	174.3	210.4	336.6
	800	130.9	137.3	143.5	152.9	173.5	191.9	345.6
C	600	167.4	177.2	186.7	201.3	233.9	263.2	336.8
	700	157.1	166	174.4	187.5	216.4	216.7	312.4
	800	166.6	176.1	185.2	199.3	230.5	189.9	272

Note: \*1 average size of 1 % of the largest drops. \*2 maximum drop size experimentally observed.

### 3. Results and Discussion

#### 3.1 Multifractal exponent - effect of internal intermittency

The maximum drop sizes estimated by the above-mentioned procedure were correlated with the impeller Weber number using Eq(3), and the multifractal exponents  $\alpha_{FT}$  were evaluated for each region. The calculated exponents  $\alpha_{FT}$  are presented in Table 4 and graphically in Figure 3. As expected, the method used for the estimation of  $d_{\text{max}}$  also significantly affects the  $\alpha_{FT}$  estimation for systems agitated by the high-shear sawtooth impeller. Therefore, the multifractal exponent  $\alpha_{FT}$  was estimated by extrapolating partial values to a cumulative 100 % value.

Table 4: The effect of the method of estimating the maximum drop size on the multifractal exponent

Region	$d_{95}$	$d_{97}$	$d_{99}$	$d_{99.3}$	$d_{99.5}$	$d_{99.7}$	$d_{99.9}$	$d_{99\text{avg}}^{*1}$	$d_{100\text{extr}}^{*2}$
A	0.899	0.945	1.04	1.06	1.09	1.13	1.21	1.33	1.7
B	0.865	0.906	0.987	1.01	1.03	1.07	1.14	1.25	1.58
C	0.931	0.979	1.08	1.1	1.13	1.17	1.26	1.27	1.46

Note: \*1 average size of 1 % of the largest drops. \*2 exponent extrapolated on  $d_{100\%}$ .

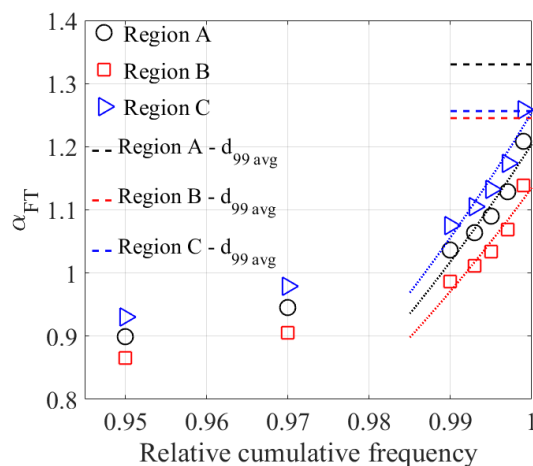


Figure 3: The multifractal exponent – effect of the method of estimating the maximum drop size

The results obtained are much more surprising and different compared to the results presented for the Rushton turbine (Formánek and Šulc, 2021). Estimating the maximum drop size  $d_{\text{max}}$  as a cumulative frequency of 97 – 99.5% the evaluated multifractal exponent  $\alpha_{FT}$  is about 1, which would indicate turbulence without internal

intermittency and droplet breakup according to theory assuming isotropic turbulence. However, estimating  $d_{max}$  as the droplet size value for 99.7% and above the cumulative frequency, the values of the multifractal exponent  $\alpha_{FT} > 1$  were obtained, which would indicate lower turbulent stresses generated by the acting eddies than predicted by the Kolmogorov theory. The regional evaluation is also interesting. The values of the multifractal exponent  $\alpha_{FT}$  are practically the same in regions A and C (the difference is about 4%). On the contrary, the values of the multifractal exponent in region B, which is above the impeller symmetrically to region A (see Figure 1), are systematically lower compared to region A and about 8% lower than in region C.

**3.2 Relation between Sauter mean diameter  $d_{32}$  and maximum drop size  $d_{max}$**

The ratio of the Sauter mean diameter  $d_{32}$  and the maximum drop size  $d_{max}$  was calculated according to Eq(2) for the maximum drop sizes estimated from the cumulative frequency drop size distribution. The calculated ratios are presented in Table 5 and the selected values are presented graphically in Figure 4.

Table 5: Proportionality constant  $C_2$  evaluated for  $d_{max}$  estimated from the cumulative frequency drop size distribution

Region	N (min <sup>-1</sup> )	$d_{99}$	$d_{99.3}$	$d_{99.5}$	$d_{99.7}$	$d_{99.9}$	$d_{99.9}^{*1}$
A	600	0.82	0.77	0.74	0.69	0.59	0.46
	700	0.8	0.76	0.73	0.68	0.59	0.47
	800	0.76	0.72	0.69	0.64	0.55	0.5
B	600	0.86	0.82	0.78	0.73	0.63	0.5
	700	0.85	0.8	0.77	0.72	0.64	0.53
	800	0.8	0.76	0.73	0.68	0.6	0.55
C	600	0.76	0.72	0.68	0.63	0.55	0.49
	700	0.7	0.67	0.64	0.6	0.51	0.51
	800	0.63	0.6	0.56	0.53	0.45	0.55

Note: \*1 average size of 1 % of the largest drops.

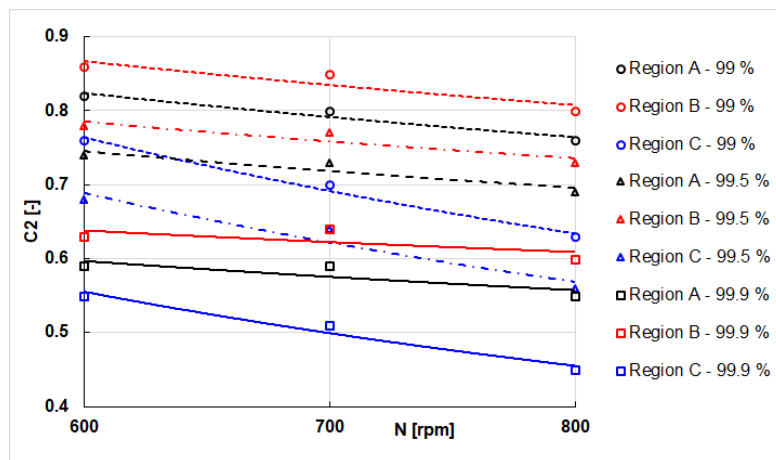


Figure 4: The dependence of proportionality constant  $C_2$  on impeller rotational speed

Table 6: Constant of proportionality  $C_2$  – hypothesis testing

	Region A			Region B			Region C		
	$d_{99}$	$d_{99.5}$	$d_{99.9}$	$d_{99}$	$d_{99.5}$	$d_{99.9}$	$d_{99}$	$d_{99.5}$	$d_{99.9}$
Relation: $\beta_{calc}$ (-)	-0.261	-0.230	0.238	-0.247	-0.261	-0.163	-0.649	-0.629	-0.692
Hypothesis: $\beta_{pred}$ (-)	0	0	0	0	0	0	0	0	0
t-characteristics  t	4.1	2.5	1.6	2.3	4.1	1	8.9	6.1	5.4
Hypothesis	Accept.	Accept.	Accept.	Accept.	Accept.	Accept.	Accept.	Accept.	Accept.
Average	0.793	0.720	0.577	0.837	0.760	0.623	0.697	0.627	0.503

Note: the critical t-distribution coefficient  $t(m-2, \alpha)$  for the significance level  $\alpha = 0.05$  is 12.706. Accept. = hypothesis is acceptable.

The effect of the impeller rotational speed  $N$  on the proportionality constant  $C_2$  was tested by hypothesis testing (Bowerman and O'Connell, 1997) for all regions investigated. The power-law dependence of the proportionality constant  $C_2$  on the impeller rotational speed was assumed as follows:  $C_2 = B_R \cdot (N)^{\beta_{\text{calc}}}$ . The independence of the proportionality constant  $C_2$  from the impeller rotational speed was formulated as the hypothesis, that is,  $C_2 = B_H \cdot (N)^0 = \text{const.}$ , i.e.  $\beta_{\text{pred}} = 0$ . The principle of this statistical method is testing of the relevance of the difference between the values of the predicted parameter and parameter evaluated from the measured data, i.e. between  $\beta_{\text{pred}}$  and  $\beta_{\text{calc}}$  respectively in this case. The results of the hypothesis testing are presented in Table 6. For illustration, the values of calculated  $|t|$  values are presented here. Despite the visual observance implies a possible dependence of the constant  $C_2$  on the impeller speed, the hypothesis test does not confirm this dependence. However, it should be noted that the number of data is small. On the other hand, the  $t$ -characteristic values are low except for region C.

#### 4. Conclusions

The effect of intermittent turbulence on drop size was analysed in a model system of immiscible silicon oil-water dispersion mechanically agitated by a high-shear sawtooth impeller in three different regions. The procedure proposed by Formánek and Šulc (2022) was adopted for the estimation of the maximum drop size. The correct determination of maximum drop size was found to be a crucial factor for the correct estimation of the multifractal exponent  $\alpha_{\text{FT}}$  for systems agitated by high-shear sawtooth impeller also. The  $\alpha_{\text{FT}}$  values of approximately 1.64 on average and 1.46 were found for regions close to the impeller and the region outside the impeller, respectively. These values would indicate smaller turbulent stresses generated by the acting eddies than predicted by the Kolmogorov theory. Finally, the relationship between the Sauter mean diameter  $d_{32}$  and the maximum drop size  $d_{\text{max}}$  was investigated. The  $d_{32}/d_{\text{max}}$  ratios of approximately 0.6 on average and 0.5 were found for regions close to the impeller and the region outside the impeller, respectively.

#### Acknowledgements

This work was supported by the Ministry of Education, Youth, and Sports of the Czech Republic under grant number RVO:12000 "R&D institutional support".

#### References

- Baldyga J., Bourne J.R., 1993, Drop Breakup and Intermittent Turbulence, *Journal of Chemical Engineering of Japan*, 26(6), 738–741.
- Baldyga J., Bourne J.R., 1995, Interpretation of turbulent mixing using fractals and multifractals, *Chemical Engineering Science*, 50(3), 381–400.
- Baldyga J., Podgórska W., 1998, Drop break-up in intermittent turbulence. Maximum stable drop size and transient sizes of drops, *Can. J. Chem. Eng.*, 76, 456–470.
- Bowerman B.L., O'Connell, R.T., 1997, *Applied statistics: improving business processes*. Richard D. Irwin, USA.
- Calabrese R.V., Chang T.P.K., Dang, P.T., 1986, Drop breakup in turbulent stirred-tank contactors. Part I: Effect of dispersed-phase viscosity, *AIChE J*, 32, 657–666.
- Formánek R., Kysela B., Šulc R., 2019, Drop Size Evolution Kinetics in a Liquid-liquid Dispersions System in a Vessel Agitated by a Rushton Turbine, *Chemical Engineering Transactions*, 74, 1039-1044.
- Formánek R., Šulc R., 2020, The Liquid-Liquid Dispersion Homogeneity in a Vessel Agitated by a High-Shear Sawtooth Impeller, *Processes*, 8, article 1012.
- Formánek R., Šulc R., 2021, The homogeneity of immiscible liquid-liquid dispersion in a vessel agitated by Rushton turbine, *Chemical and Process Engineering*, 42(3), 209-222.
- Hinze J.O., 1955, Fundamentals of the hydrodynamic mechanism of splitting in dispersion processes, *AIChE J.*, 1, 289-295.
- Kolmogorov A.N., 1949, The breakage of drops in a turbulent current, *Dokl. Akad. Nauk SSSR*, 66, 825–828.
- Meneveau C., Sreenivasan K. R., 1989, Measurement of  $f(\alpha)$  from scaling of histograms, and applications to dynamical systems and fully developed turbulence. *Physics Letters A*, 137(3), 103–112.
- Meneveau C., Sreenivasan K. R., 1991, The multifractal nature of turbulent energy dissipation. *Journal of Fluid Mechanics*, 224, 429–484.
- Pacek A.W., Man C.C., Nienow A.W., 1998, On the Sauter mean diameter and size distributions in turbulent liquid/liquid dispersions in a stirred vessel, *Chem Eng Sci*, 53(11), 2005-2011.
- She Zhen-Su, Leveque E., 1994, Universal scaling laws in fully developed turbulence. *Physical Review Letters*, 72(3), 336–339.